Research on Engineering Structures & Materials
www.jresm.org
Research Group

Research Article

System-level performance and association policy evaluation of a BIM-derived indoor IEEE 802.11ax deployment under variable user density

Emsal Altınay [*,1,2,a], Ecir Uğur Küçüksille [2,b], Duygu Köse Uçar [3,c]

[1]*Dept. of Information Technology, Isparta University of Applied Sciences, Isparta, Türkiye*
[2]*Dept. of Computer Engineering, Engineering Faculty, Süleyman Demirel University, Isparta, Türkiye*
[3]*Dept. of Architecture, Faculty of Architecture, Süleyman Demirel University, Isparta, Türkiye*

Article Info

Article History:

Received 08 Oct 2026
Accepted 13 Nov 2026

Keywords:

Indoor Wi-Fi;
IEEE 802.11ax;
Building Information Modeling;
AP association;
Load balancing;
System-level simulation

Abstract

This study presents a controlled system-level benchmark of a Building Information Modeling (BIM)-derived indoor IEEE 802.11ax deployment under variable user density and access-point (AP) association policy. Four fixed APs, inherited from a preceding radio-frequency (RF) coverage optimization, were evaluated with 10, 30, 50, and 70 static stations under received signal strength indicator (RSSI), load-aware, and hybrid association. The primary benchmark used fixed modulation and coding scheme (MCS) 4 with link adaptation disabled, 2.4 GHz/20 MHz operation, a fixed 1-6-11-1 channel plan, and downlink full-buffer traffic. Since BIM wall mapping was partial, an empirical fallback of 50 dB/m was applied to unmapped segments, and this assumption was tested in a low-loss foam sensitivity analysis. Across 120 paired-topology runs, association policy did not significantly change aggregate throughput (p=0.111), but it strongly affected Jain fairness, station-count load imbalance, and serving RSSI. At 70 stations, all policies entered a functional congestion collapse, with approximately 62% mean packet loss and 15% zero-throughput users. Supplementary analyses indicated that station-count balance alone was not sufficient to infer per-AP delivered-throughput balance under saturated traffic, while a three-seed bidirectional bursty test preserved the same qualitative policy ordering. The results support load-aware association as a resource-distribution mechanism, but not as a remedy for configuration-specific saturation or RF-coverage limitations.

© 2026 MIM Research Group. All rights reserved.

1. Introduction

In a wireless local area network (WLAN) with several access points (APs), a station's strongest received signal does not necessarily identify the AP best placed to accommodate another active user. As more stations share the same infrastructure, the association decision affects how demand is divided among APs. IEEE 802.11ax introduced orthogonal frequency-division multiple access (OFDMA), multi-user transmission, and spatial-reuse mechanisms to improve operation in dense WLANs [1-4]. These mechanisms address radio access, but do not by themselves determine which AP a station should select.

The shortcomings of strongest-signal association have been studied across several WLAN generations. Vasudevan et al., Bejerano et al., and Gong and Kim examined AP selection, association control, load distribution, and fairness [5-7]. Subsequent work considered both radio quality and measured or estimated load [8,9]. For IEEE 802.11ax, Ak and Canberk investigated quality-of-service (QoS)-aware load balancing [10]. Studies of IEEE 802.11be have also examined controller-assisted multi-link operation and cooperative resource allocation [11,12]. These two address

*Corresponding author: emsalaltinay@isparta.edu.tr
[a]orcid.org/0000-0002-0315-0894, [b]orcid.org/0000-0002-3293-9878, [c]orcid.org/0000-0002-1643-0510
DOI: http://dx.doi.org/10.17515/resm2026-2450ce1008rs

network resource management, not a station-count association rule like the one tested here, so they give context but no direct evidence on the HYBRID policy.

Association also depends on which APs offer a usable link at a given location. Distance, wall placement, building materials, and frequency all shape indoor signal attenuation [13-18]. Recent work covers Wi-Fi 6E deployment at 6 GHz [19] and Building Information Modeling (BIM)-assisted RSS prediction, AP placement, and indoor positioning [20-22]. In these BIM studies, the model supplies the geometry and material information required for site-specific prediction. Here, the BIM data provide the floor boundary and the layered wall descriptions used in the propagation calculations.

This study takes the AP layout as given. The four AP positions come from a preceding BIM-based radio-frequency (RF) coverage optimization. In the present system-level benchmark, the AP configuration and channel assignments remain fixed, while station density and association policy vary. The study does not propose a new placement algorithm or attempt to evaluate the full range of dynamic IEEE 802.11ax features. Instead, it examines how RSSI-based, load-aware, and HYBRID association policies affect aggregate throughput and the distribution of service among users and APs as station density increases.

The main comparison covers aggregate throughput, user fairness, serving RSSI, and association-count imbalance at 10, 30, 50, and 70 stations under fixed-MCS, 2.4 GHz, saturated downlink traffic, and it checks whether uneven station assignment shows up in delivered traffic. Three supplementary analyses address assumptions that the main matrix cannot test: the wall-loss value for polystyrene foam, per-AP throughput balance, and a small bidirectional On-Off traffic scenario.

2. Material and Method

2.1 Study Design and Simulation Environment

The main experiment used four station densities, three association rules, and ten random seeds per density, for 120 simulations. Within a given density and seed, the same station coordinates were used for RSSI, LOAD, and HYBRID association. AP locations and channel assignments were also unchanged. Consequently, policy comparisons are paired by spatial realization rather than confounded by different random placements of stations.

The baseline is deliberately narrower than a full dynamic Wi-Fi 6 evaluation. Stations are static, MCS 4 is fixed with link adaptation disabled, operation is limited to 2.4 GHz with 20 MHz channels on a fixed 1-6-11-1 plan, and the main traffic model is saturated downlink full-buffer traffic. These controls isolate the effects of density and association, but they also limit what the outage, packet-loss, and saturation results can be taken to mean.

The network was implemented in MATLAB R2026b using WLAN Toolbox and Wireless Network Toolbox. The system-level framework used IEEE 802.11ax High Efficiency (HE) capability, an abstract physical layer (PHY) based on the Task Group ax (TGax) evaluation methodology, and a full medium access control (MAC) and frame-abstraction configuration for the primary benchmark [23,24]. The main simulation parameters are listed in Table 1.

2.2 BIM-Derived Study Area and Preceding AP Placement

The study area was extracted from an Autodesk Revit model. The two-dimensional analysis boundary was formed from the floor extents containing the four APs, and the wall segments at the study level were exported with their thickness, height, and layer information. The geometry served both to constrain random STA placement and to test wall intersections along each AP-STA path. The numerical boundary polygon, wall segments, wall thicknesses, layer descriptions, and AP coordinates used by the simulator are provided as supplementary CSV data. The coordinates are local Cartesian values read directly by the MATLAB geometry functions. The extracted geometry and AP layout are shown in Fig. 1, and Table 2 lists the AP coordinates and channels.

Table 1. Main simulation parameters

Parameter	Configuration
WLAN capability	IEEE 802.11ax HE
Frequency band	2.4 GHz
Channel bandwidth	20 MHz
APs	4
AP transmit power	24 dBm
STA transmit power	15 dBm
MCS / rate control	4 / fixed; link adaptation disabled
PHY model	Abstract PHY based on TGax evaluation methodology
MAC model	Full MAC with frame abstraction
Primary traffic	Downlink full-buffer
User densities	10, 30, 50, 70 STAs
Association policies	RSSI, LOAD, HYBRID
HYBRID α	0.30
Eligibility threshold	−70 dBm
Simulation duration	20 s
Paired random seeds	10
Spatial streams	1 (WLAN Toolbox default; not overridden)
Guard interval	Not explicitly configured; toolbox-managed (effective value not separately logged)
A-MPDU aggregation	WLAN Toolbox HE defaults; no custom aggregation limit
UL / DL OFDMA	Disabled (default; neither enabled explicitly)
BSS coloring / spatial reuse	Disabled (BSSColor = 0, default)

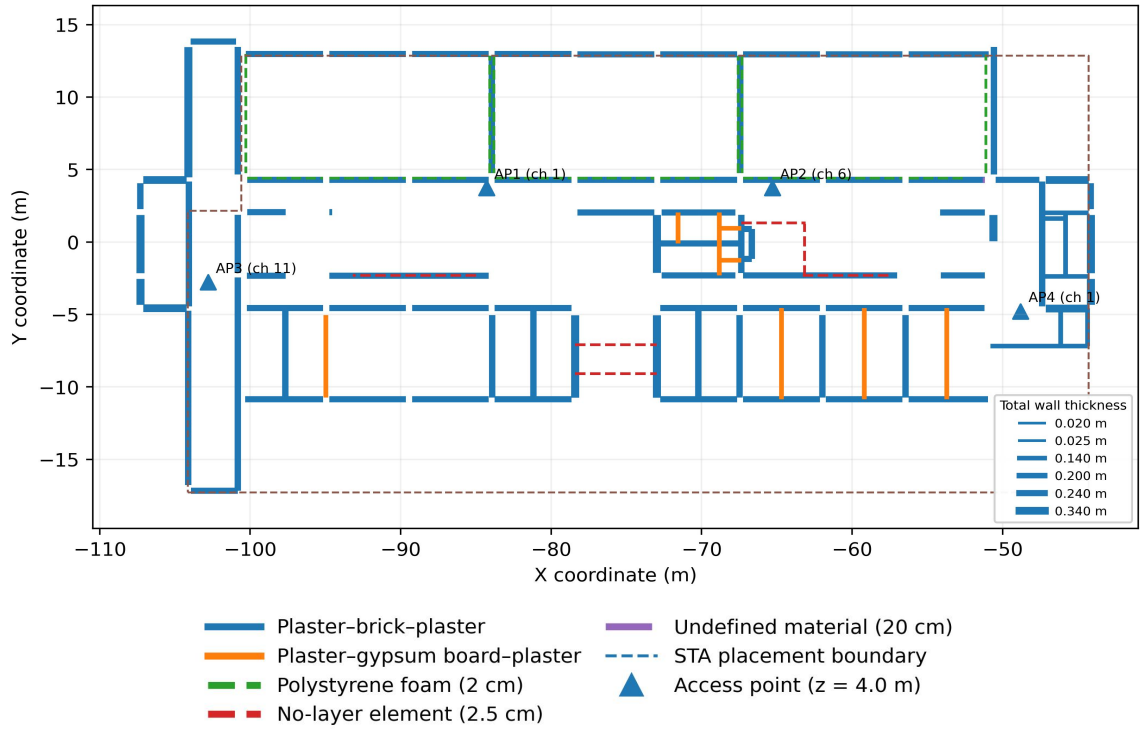


Fig. 1. BIM-derived floor geometry and fixed AP layout. Line color and style identify the wall material class; the line-width key reports total BIM wall thickness. Exact segment geometry, layer descriptions, and fallback assignments are supplied in the supplementary CSV files

The four AP x-y coordinates were inherited from a preceding ant colony optimization (ACO) placement stage run on the same BIM floor geometry. That stage optimized spatial RF coverage, defined as the proportion of evaluation-grid points with predicted RSSI ≥ −70 dBm, rather than

multi-user traffic performance. The selected layout reached 95.2% simulated coverage, a 3.0% dead-zone fraction, 55.1% redundancy, a mean RSSI of −43.2 dBm, and a fitness value of 0.9377. These figures were obtained with the placement stage's own propagation model, whose material-loss parameters differ from those used here, so they are not claimed to hold for the benchmark. Multi-user contention, association policy, packet loss, and fixed-MCS outage were not objectives of that stage. Its optimizer settings are outside the scope of this article, which uses the stage only as the source of the four AP coordinates. In this article, “optimized” therefore refers only to the RF-coverage objective and not to operational throughput.

The placement stage returned x-y coordinates but no mounting height, so all APs were assigned a height of 4.0 m, the BIM ceiling plane, and STAs were placed at 1.2 m. In the exported geometry, 90 of the 120 wall segments end at 4.0 m, 21 lower, and 9 higher. The 4.0 m value is a modeling assumption, not an optimized or field-verified mounting height. The propagation model uses the 3D Euclidean AP-STA distance and a vertical check on wall intersections, but it is not a ray tracer and does not model floor or ceiling reflections, diffraction, inter-floor propagation, or explicit multipath.

Table 2. Fixed AP positions and channel allocation

AP	X (m)	Y (m)	Z (m)	Channel
AP1	−84.30	3.72	4.00	1
AP2	−65.30	3.72	4.00	6
AP3	−102.80	−2.78	4.00	11
AP4	−48.80	−4.78	4.00	1

2.3 BIM-Based Indoor Propagation Model

For each AP-STA link, the model adds BIM-derived wall penetration losses to a distance-dependent term adapted from the IEEE TGax indoor simulation scenarios [25]. ITU-R P.2040 and the measurement studies [16-18] support the dependence of transmission and reflection on material and frequency, but they do not supply the dB/m coefficients used here. These coefficients are effective, study-specific parameters of this simulation, not measured material constants. The total path loss is expressed as:

$$PL_{total} = PL_{distance} + \sum_{w} L_w \tag{1}$$

$$PL_{distance} = 40.052 + 20\ log_{10}\left(\frac{f_c}{2.4}\right) + 20\ log_{10}[min(d,5)] + I(d>5)\ 35\ log_{10}\left(\frac{d}{5}\right) \tag{2}$$

where f_c is the channel center frequency in GHz, d is the 3D Euclidean transmitter-receiver distance in meters, and $I(d>5)$ is an indicator equal to one when d exceeds 5 m. A minimum distance of 1 m was used for numerical stability. For a crossed wall, the layer loss is:

$$L_w = \sum_{l} a_l t_l \tag{3}$$

where a_l is the effective coefficient assigned to layer l and t_l is the orthogonal BIM layer thickness. The mapped coefficients were 100 dB/m for concrete, 60 dB/m for brick, 25 dB/m for gypsum board, and 50 dB/m for plaster. As an example, a wall made of 20 mm plaster, 200 mm brick, and 20 mm plaster loses 14 dB under these coefficients. The mapped layers among the 120 study-level walls are plaster, brick, and gypsum board. Because no concrete layer occurred, the 100 dB/m coefficient was not used in this study area. The Loss_dB column of the supplementary walls.csv reproduces these values for all 98 mapped walls. The implementation uses the orthogonal thickness and does not replace t_l by $t_l/\cos\theta$ (θ being the angle of incidence) for oblique incidence, nor does it add an angle-dependent reflection loss. This simplification is a limitation: Eq. (3) is not a complete electromagnetic wall model.

Of the 120 study-level walls, 98 were mapped directly from BIM layer descriptions. The other 22 could not be mapped: 15 polystyrene-foam segments, six elements with no layer information, and one element of undefined material. The baseline model gave these elements an empirical fallback

of 50 dB/m. Because the affected layers are thin, the fallback adds 1.0 dB per foam segment (2 cm), 1.25 dB per no-layer element, and 10 dB for the single undefined 0.2 m element (supplementary file walls_fallback_audit.csv); at 1 and 3 dB/m a foam segment would add only 0.02 and 0.06 dB. Direct 2.4 GHz measurements of common construction materials, including foamed polystyrene, reported relatively good transmission for most of the materials tested [18]. The 15 foam segments were therefore re-evaluated with low-loss sensitivity bounds of 1 and 3 dB/m. Neither value is presented as an intrinsic material constant.

Relative to the 50 dB/m baseline, the low-loss foam sensitivity changed association decisions for approximately 0.12% of station realizations under RSSI, 4.23% under LOAD, and 3.13% under HYBRID. The mean RSSI at the original serving AP changed by about 0.17–0.20 dB, individual links by up to 2.82–2.94 dB, and candidate-AP eligibility sets in approximately 0.97% of realizations. The 1 and 3 dB/m bounds gave almost identical change rates. Within the adopted propagation model, the baseline fallback can therefore create localized shadowing that matters mainly for decisions based on an RSSI eligibility threshold.

For each AP-STA link, the two-dimensional propagation segment was tested against every wall segment. A wall loss was included only when the corresponding intersection also lay within the actual vertical extent of that wall. This prevents a plan-view crossing from being counted when the three-dimensional ray passes above or below the wall.

2.4 Station Topology and Traffic Models

STA locations were drawn from a uniform random distribution inside the study-area polygon at densities of 10, 30, 50, and 70 users, and stations remained static during each run. Uniform sampling serves as a neutral paired baseline because it places no hotspot near any particular AP. It does not capture room-level clustering of occupants, and the lack of hotspot or clustered user processes is a limitation of this benchmark.

The primary runs used saturated downlink full-buffer traffic. This gives a reproducible stress benchmark, but it is not representative of asynchronous web, video, or voice traffic, and application latency is not interpreted from these runs. To see whether the ordering of the policies survives outside this unidirectional saturated baseline, a supplementary 50-STA experiment used simultaneous bidirectional On-Off traffic, with 4 Mbps downlink and 1 Mbps uplink during 0.5 s ON periods followed by 0.5 s OFF periods. The supplementary On-Off test used full MAC processing instead of the primary benchmark's full MAC with frame abstraction; traffic-profile effects therefore cannot be isolated. Only three paired seeds were run, and the results are descriptive rather than confirmatory. Mobility, re-association, handover overhead, and application-specific web, video, and VoIP traffic remain outside the scope of this study.

2.5 AP Association Strategies

2.5.1 RSSI-Based Association

Under RSSI association, station i was assigned to the AP j with the largest calculated received signal strength $RSSI_{ij}$. This strongest-signal baseline corresponds to the conventional association behavior discussed in prior AP-selection studies [5-9]:

$$AP_i^* = \arg\max_j RSSI_{ij} \tag{4}$$

2.5.2 Load-Aware Association

Under LOAD association, stations were processed in ascending order of their strongest available AP RSSI. For each station, the eligible set consisted of the APs with RSSI ≥ −70 dBm, and the station was assigned to the eligible AP with the fewest currently associated STAs. Ties were broken by RSSI. If no AP satisfied the threshold, the strongest-RSSI AP was used. L_j is only a station-count load proxy: it does not measure airtime utilization, channel occupancy, or spectral-resource consumption, and it cannot by itself establish MAC-layer load balance.

2.5.3 Hybrid Association

The HYBRID strategy combined normalized RSSI and the same station-count proxy. The normalization and weighting equations below were defined for this study. Combining the two terms follows earlier AP-selection work in which RSSI was combined with channel-load information [9]. RSSI was normalized with fixed bounds of −70 and −30 dBm, which are $RSSI_{min}$ and $RSSI_{max}$ in Eq. (5):

$$R_{ij}^{norm} = \frac{RSSI_{ij} - RSSI_{min}}{RSSI_{max} - RSSI_{min}} \tag{5}$$

The normalized AP station-count proxy is:

$$L_j^{norm} = min\left[\frac{L_j}{max\left(\underset{k}{max}L_k, 1\right)}, 1\right] \tag{6}$$

and the hybrid score is:

$$S_{ij} = \alpha\, R_{ij}^{norm} + (1 - \alpha)\left(1 - L_j^{norm}\right) \tag{7}$$

Only APs with RSSI ≥ −70 dBm were scored, and normalized RSSI was clipped to [0, 1], which affects only links stronger than −30 dBm. Stations were processed in the same order as under LOAD association, and a station with no eligible AP was assigned to its strongest-RSSI AP. The AP with the largest score was selected, and RSSI broke score ties. The final weight α=0.30 was fixed before the main experiment. A preliminary screening compared α={0.30, 0.50, 0.60, 0.70}, and the two leading candidates were then evaluated with five paired seeds and 20-s runs. Relative to α=0.50, α=0.30 reduced AP-load variation and improved fairness with less than a 1% reduction in mean aggregate throughput, so it was retained for the main experiment. To separate association-count balance from delivered-traffic balance, $CV_{throughput}$, the coefficient of variation of per-AP delivered application throughput, is also reported for the 50- and 70-STA supplementary runs.

2.6 Simulation-Duration Selection and Experimental Matrix

A duration-convergence check used 50 STAs with HYBRID association at 0.5, 1, 2, 5, 10, and 20 s. Aggregate throughput increased from 4.10 Mbps at 0.5 s to 139.76 Mbps at 10 s and 144.37 Mbps at 20 s, while Jain fairness changed from 0.741 to 0.748 between 10 and 20 s. The publication duration was therefore fixed at 20 s. The main matrix comprised four densities, three association policies, and ten paired seeds, producing 120 runs. These are not 120 independent spatial topologies: each density-seed topology is reused across the three policies.

2.7 Performance Metrics

User throughput T_i was calculated from application-layer received bytes B_i over simulation duration t:

$$T_i = \frac{8\, B_i}{(t \times 10^6)} \tag{8}$$

Aggregate throughput is the sum of user throughputs. Mean user throughput and the fifth and tenth percentiles (P05 and P10) were also calculated. P10 is emphasized because P05 often collapsed to zero under dense fixed-MCS operation. ZeroThroughputRatio is the fraction of stations with throughput ≤10^{-6} Mbps. User fairness is quantified using the Jain index [26], with n denoting the number of stations:

$$J = \frac{\left(\sum_{i=1}^{n} T_i\right)^2}{n \sum_{i=1}^{n}\left(T_i^{\,2}\right)} \tag{9}$$

Station-count imbalance is represented by the coefficient of variation of the number of associated users. The coefficient of variation is the standard deviation divided by the mean [27], here

computed over the four APs, where σ_L and $\bar{L}$ denote the sample standard deviation (divisor 3 for the four APs) and the mean of L_j:

$$CV_{load} = \frac{\sigma_L}{\bar{L}} \quad (10)$$

Lower CV_{load} indicates a more even association-count distribution, but not necessarily equal airtime or throughput. The secondary metric $CV_{throughput}$ applies the same definition to delivered throughput, aggregated separately for each AP. Mean packet-loss ratio, mean and minimum serving RSSI, and AP minimum/maximum association counts were also recorded.

The reported mean packet-loss ratio measures application-layer non-delivery over 20 s. For each station, it equals one minus the STA application-layer received-packet count divided by the destination-specific AP application-layer transmitted-packet count, clipped to [0, 1]. The mean averages station ratios with positive transmitted counts rather than pooling network totals. It does not separate MAC retry-limit drops, queue overflow, or packets still queued or in transit at termination.

2.8 Statistical Analysis

Because the three association policies use the same topology for each density and seed, association and density were treated as repeated factors, with seed as the repeated experimental subject. Two-factor repeated-measures analysis of variance (ANOVA) was applied to the principal outcomes. Both factors have more than two levels, so Greenhouse-Geisser-corrected degrees of freedom and p-values are reported to reduce sensitivity to violations of sphericity [28]. For each outcome, paired t tests compared RSSI-LOAD, RSSI-HYBRID, and LOAD-HYBRID within each of the four density levels. The reported Holm-adjusted primary contrasts correspond to a family of twelve within-density policy comparisons per outcome (three pairs at each density) [29]. Partial eta squared (ηp^2) is reported for omnibus effects and Cohen d_z for paired contrasts. Group summaries are reported as mean ± standard deviation, 95% confidence intervals (CIs) are used in figures and selected contrasts, and $p<0.05$ was the significance threshold. The five-seed per-AP-throughput and three-seed bursty-traffic analyses are supplementary. The latter is interpreted descriptively because it has so few paired topologies.

3. Results

3.1 Aggregate Network Throughput and Configuration-Specific Saturation

Aggregate throughput increased between 10 and 30 STAs and then remained between 145.24 and 148.59 Mbps. At 10 STAs, mean aggregate throughput was 134.56 Mbps under RSSI, 141.44 Mbps under LOAD, and 141.39 Mbps under HYBRID. At 30 STAs, the corresponding values were 145.69, 145.90, and 146.76 Mbps. At 50 STAs, they were 147.69, 145.24, and 146.89 Mbps, and at 70 STAs, 147.44, 147.28, and 148.59 Mbps (Fig. 2).

The association main effect was not significant, $F(1.17,10.56) = 2.96$, $p=0.111$, $\eta p^2=0.247$. Density was also not significant after Greenhouse-Geisser correction, $F(1.19,10.75)=2.08$, $p=0.178$, $\eta p^2=0.188$, and neither was the Association×Density interaction, $F(1.13,10.13)=2.37$, $p=0.154$, $\eta p^2=0.208$. No HYBRID-RSSI throughput contrast remained significant after Holm adjustment. The 145–149 Mbps plateau at 30–70 STAs is read as a saturation ceiling of this configuration (fixed 2.4 GHz/20 MHz channels, full-buffer traffic, fixed MCS). It does not show that the physical deployment is intrinsically resilient at high density.

3.2 User Fairness

Association policy made a larger difference to Jain fairness. RSSI yielded mean values of 0.630, 0.606, 0.677, and 0.707 at 10, 30, 50, and 70 STAs. HYBRID produced 0.716, 0.775, 0.810, and 0.810, while LOAD remained close to HYBRID (Fig. 3). The main effect of association on Jain fairness was significant, $F(1.02,9.14)=21.42$, $p=0.0012$, $\eta p^2=0.704$. Density, $F(1.53,13.74) = 2.66$, $p=0.115$, $\eta p^2=0.228$, and the association × density interaction, $F(1.61,14.52) = 1.28$, $p=0.300$, $\eta p^2=0.124$, were not significant. HYBRID exceeded RSSI by 0.168 at 30 STAs (95% CI 0.064–0.273; Holm $p=0.043$; $d_z=1.154$), 0.133 at 50 STAs (95% CI 0.064–0.202; Holm $p=0.018$; $d_z=1.378$), and by 0.103

at 70 STAs (95% CI 0.063–0.143; Holm p=0.003; d_z=1.833). HYBRID and LOAD did not differ significantly in fairness.

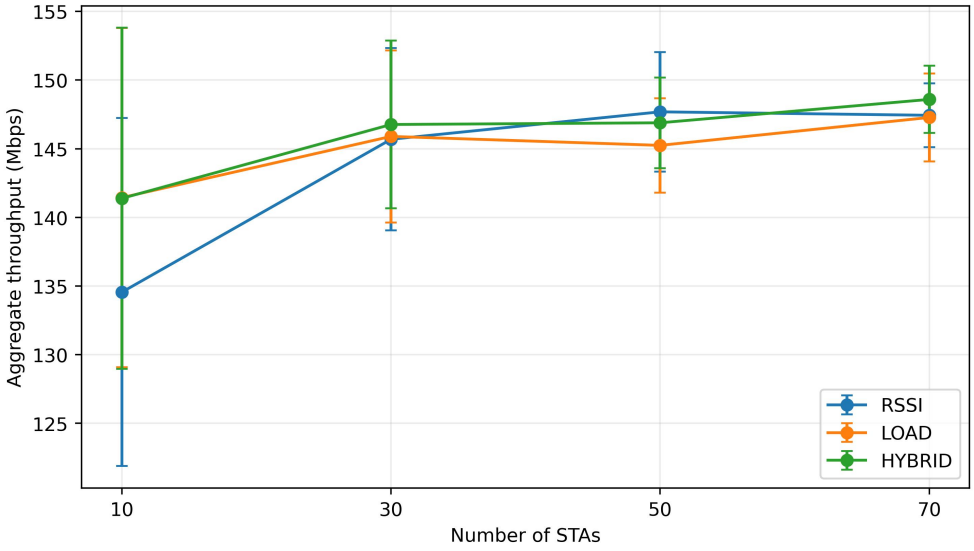


Fig. 2. Aggregate throughput versus the four simulated user-density levels. Error bars indicate 95% confidence intervals

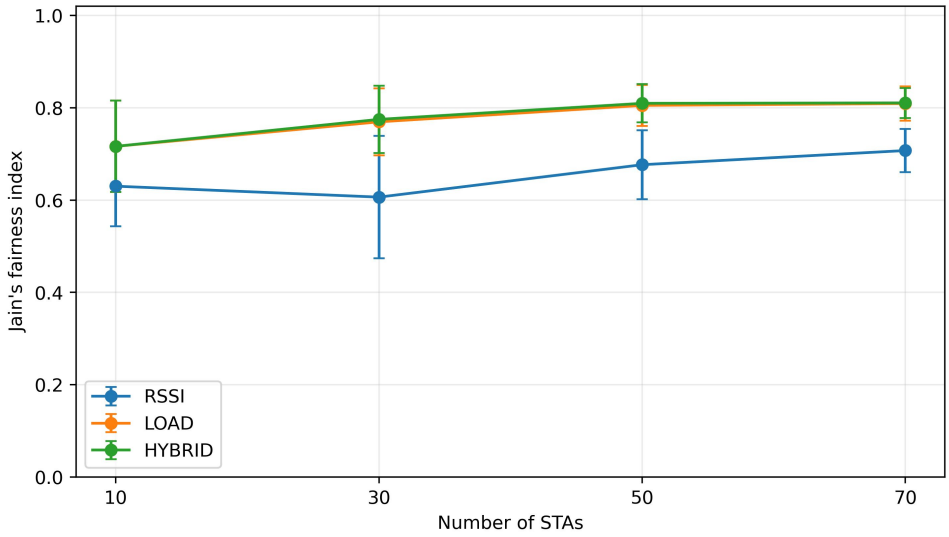


Fig. 3. Jain fairness versus the four simulated user-density levels, error bars show 95% confidence intervals

3.3 Association-Count Balance

Under RSSI, station-count CV (CV_{load}) was 0.662, 0.512, 0.474, and 0.419 for 10, 30, 50, and 70 STAs. HYBRID reduced it to 0.412, 0.194, 0.142, and 0.105, and LOAD to 0.412, 0.170, 0.078, and 0.052 (Fig. 4). Association had a strong effect, $F(1.03,9.26)=69.67$, $p<0.001$, $\eta p^2=0.886$. Density was also significant, $F(1.16,10.43)=8.41$, $p=0.013$, $\eta p^2=0.483$. The interaction was not significant, $F(1.98,17.83)=1.68$, $p=0.215$, $\eta p^2=0.157$. HYBRID had significantly lower CV_{load} than RSSI at every density after Holm correction, and LOAD was significantly lower than HYBRID at 50 and 70 STAs. At these two densities, LOAD produced the most even distribution of associated stations. These results quantify balance in association counts only. They are not a direct measure of airtime balance.

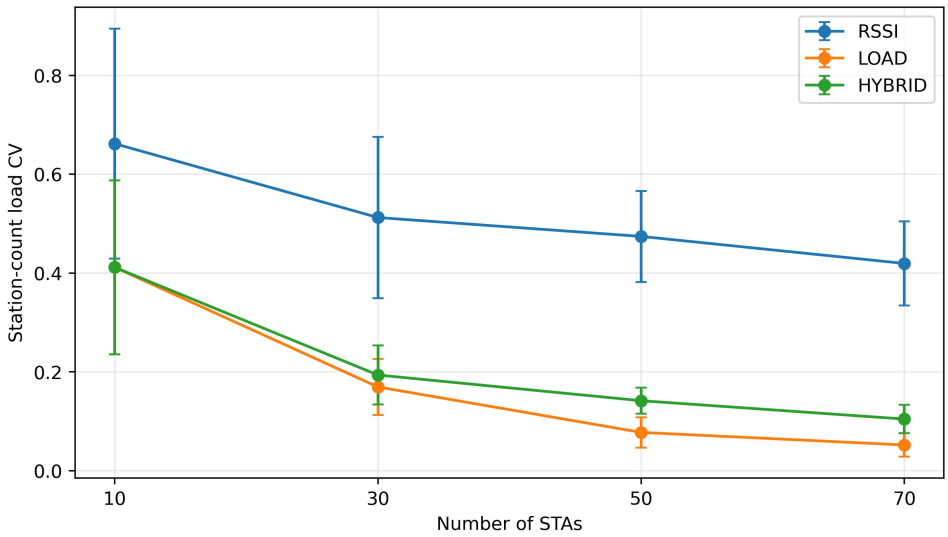


Fig. 4. Station-count load coefficient of variation versus user density, error bars show 95% confidence intervals

3.4 Packet Loss and Lower-Tail Throughput

Packet loss increased sharply with density. Under RSSI the mean loss ratio rose from 0.178 at 10 STAs to 0.350, 0.507, and 0.626 at 30, 50, and 70 STAs. HYBRID produced 0.188, 0.279, 0.483, and 0.622; LOAD produced 0.188, 0.286, 0.490, and 0.620 (Fig. 5). Association was significant, $F(1.07,9.65)=5.49$, $p=0.040$, $\eta p^2=0.379$. Density had a very large effect, $F(1.74,15.66)=101.85$, $p<0.001$, $\eta p^2=0.919$, and the interaction was significant, $F(1.98,17.79)=7.10$, $p=0.0055$, $\eta p^2=0.441$. The largest HYBRID-RSSI difference occurred at 30 STAs, where HYBRID reduced the mean loss ratio by 0.071 (95% CI −0.112 to −0.029). The Holm-adjusted p-value for the 30-STA contrast was 0.0495, narrowly meeting the $p<0.05$ criterion. This borderline result warrants cautious interpretation and does not establish a general reduction in packet non-delivery. The contrasts at 50 and 70 STAs were not statistically significant.

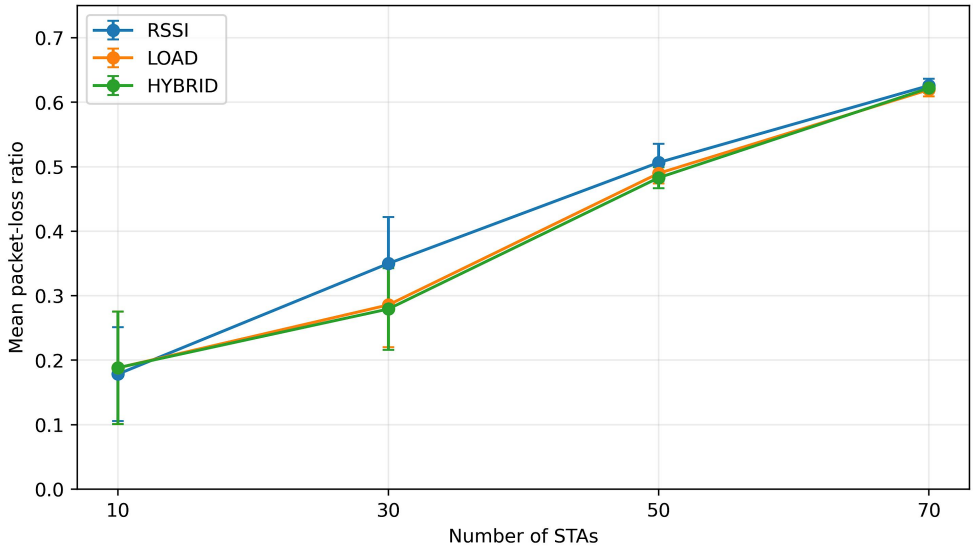


Fig. 5. Mean packet-loss ratio versus the four simulated user-density levels. Error bars show 95% confidence intervals

At 70 STAs, the application-layer packet non-delivery measure approached 62% under every policy. Together with approximately 15% zero-throughput users and a sharply reduced P10 throughput, this indicates functional congestion collapse under the simulated saturated fixed-rate

condition. The non-delivery measure does not resolve which individual packet losses arose from MAC retries, queue drops, or unfinished transmissions at the simulation boundary.

P10 throughput also collapsed as density grew. HYBRID decreased from 3.177 Mbps at 10 STAs to 0.910, 0.200, and 0.027 Mbps at 30, 50, and 70 STAs. RSSI decreased from 2.329 to 0.442, 0.129, and 0.016 Mbps (Fig. 6). The association main effect was not significant, F(1.00,9.01)=2.76, p=0.131, ηp^2=0.235. Density reached the 0.05 threshold, F(1.06,9.54)=5.11, p=0.047, ηp^2=0.362, while the interaction was not significant, F(1.21,10.87)=1.94, p=0.193, ηp^2=0.177.

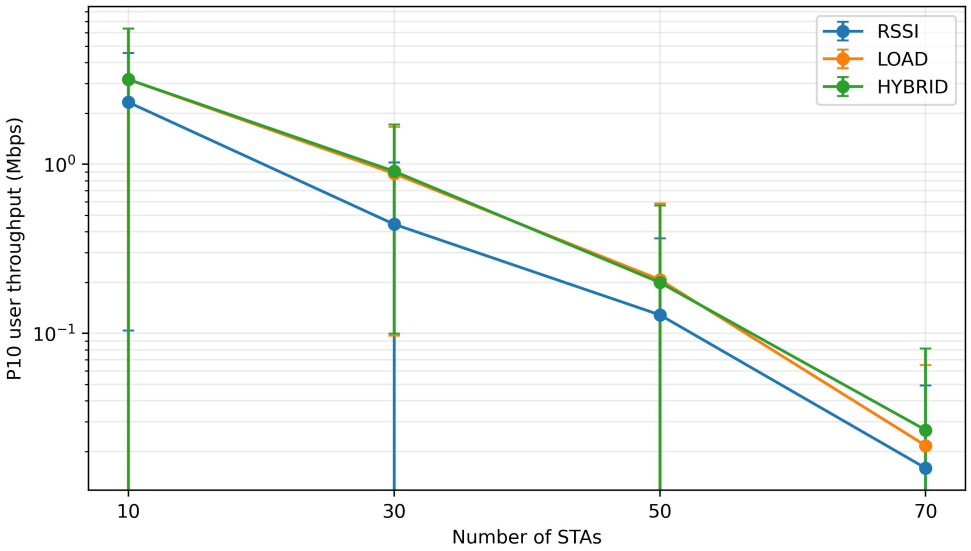


Fig. 6. P10 user throughput on a logarithmic y-axis. The x-axis contains only the four simulated user-density levels. Error bars show 95% confidence intervals. Lower limits that are zero or negative cannot be shown on a logarithmic axis, so those bars are truncated at the lower edge of the plot

3.5 Serving-Link RSSI And Zero-Throughput Users

Strongest-RSSI association produced the highest mean serving RSSI, remaining between approximately −52.4 and −53.0 dBm. HYBRID produced −55.05, −55.14, −54.65, and −55.00 dBm across increasing density. LOAD produced −55.05, −56.57, −56.28, and −56.79 dBm (Fig. 7). Association was significant, F(1.22,10.96)=59.90, p<0.001, ηp^2=0.869. Density was not significant, F(1.74,15.70)=0.27, p=0.736, ηp^2=0.029, and the interaction remained above 0.05, F(2.12,19.11)=3.27, p=0.057, ηp^2=0.267. HYBRID serving RSSI was approximately 2.0–2.5 dB weaker than that of RSSI, but at 30, 50, and 70 STAs it was 1.43, 1.63, and 1.78 dB stronger than that of LOAD. These differences remained significant after Holm correction.

The zero-throughput ratio remained similar across policies: 0.130 at 10 STAs, 0.157 at 30 STAs, 0.138 at 50 STAs, and approximately 0.147–0.149 at 70 STAs. Association, density, and their interaction were not significant. A diagnostic 10-STA RSSI run, examined after the main experiment, showed three zero-throughput users with serving RSSI of −73.70, −80.24, and −84.81 dBm and a packet-loss ratio of 1.0. This supports an outage-like interpretation under fixed MCS 4, but it should not be generalized into a universal Wi-Fi coverage threshold. None of this invalidates the preceding coverage optimization, which targeted spatial RF coverage and not multi-user service at a fixed MCS. It does show that good RF coverage by itself cannot prevent weak-link or overload outages in this configuration.

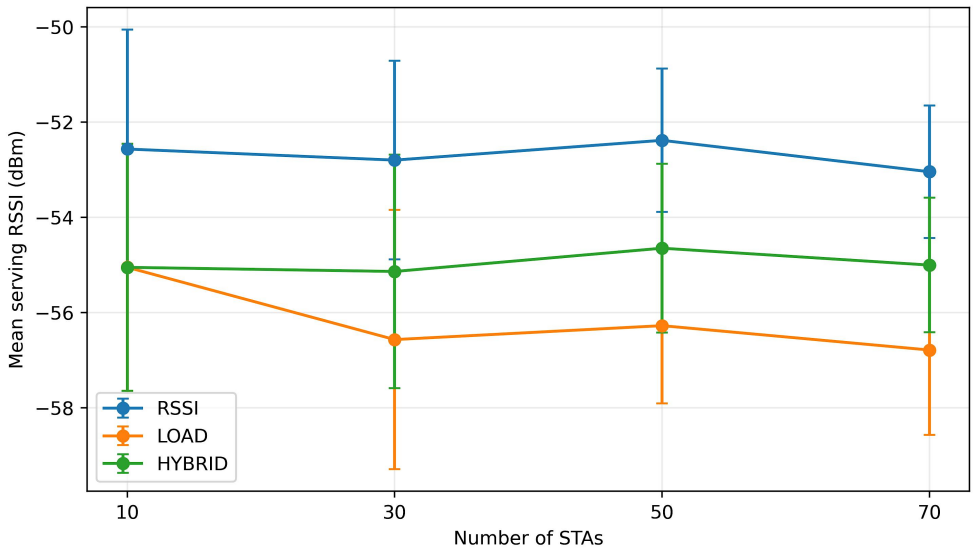


Fig. 7. Mean serving-link RSSI versus the four simulated user-density levels. Error bars show 95% confidence intervals

3.6 Descriptive Summary and Omnibus Statistics

Table 3 summarizes the main performance metrics for each density and policy, and Table 4 reports the omnibus repeated-measures tests.

Table 3. Main performance metrics for the compared association policies (mean ± standard deviation over 10 paired seeds). Count CV denotes the station-count CV (CV_{load})

STA	Policy	Agg. Mbps	Jain	Count CV
10	RSSI	134.558±17.712	0.630±0.121	0.662±0.326
10	LOAD	141.441±17.250	0.716±0.138	0.412±0.246
10	HYBRID	141.386±17.373	0.716±0.138	0.412±0.246
30	RSSI	145.686±9.285	0.606±0.185	0.512±0.228
30	LOAD	145.896±8.762	0.769±0.101	0.170±0.079
30	HYBRID	146.764±8.538	0.775±0.102	0.194±0.084
50	RSSI	147.687±6.097	0.677±0.105	0.474±0.129
50	LOAD	145.244±4.810	0.805±0.062	0.078±0.043
50	HYBRID	146.889±4.610	0.810±0.058	0.142±0.037
70	RSSI	147.435±3.258	0.707±0.066	0.419±0.119
70	LOAD	147.277±4.491	0.809±0.052	0.052±0.033
70	HYBRID	148.592±3.418	0.810±0.045	0.105±0.040
STA	Policy	Loss	P10 Mbps	RSSI dBm
10	RSSI	0.178±0.102	2.329±3.110	−52.566±3.509
10	LOAD	0.188±0.122	3.177±4.441	−55.050±3.628
10	HYBRID	0.188±0.122	3.177±4.441	−55.051±3.629
30	RSSI	0.350±0.101	0.442±0.818	−52.799±2.914
30	LOAD	0.286±0.092	0.881±1.096	−56.568±3.804
30	HYBRID	0.279±0.089	0.910±1.133	−55.138±3.427
50	RSSI	0.507±0.041	0.129±0.330	−52.383±2.104
50	LOAD	0.490±0.022	0.208±0.530	−56.276±2.280
50	HYBRID	0.483±0.023	0.200±0.517	−54.649±2.477
70	RSSI	0.626±0.015	0.016±0.047	−53.043±1.944
70	LOAD	0.620±0.014	0.022±0.060	−56.787±2.496
70	HYBRID	0.622±0.009	0.027±0.076	−55.003±1.977

Table 4. Greenhouse-Geisser-corrected repeated-measures ANOVA

Outcome	Association	Density
Aggregate throughput	$F(1.17,10.56)=2.96$, $p=0.111$, $\eta p^2=0.247$	$F(1.19,10.75)=2.08$, $p=0.178$, $\eta p^2=0.188$
Packet loss	$F(1.07,9.65)=5.49$, $p=0.040$, $\eta p^2=0.379$	$F(1.74,15.66)=101.85$, $p<0.001$, $\eta p^2=0.919$
Jain fairness	$F(1.02,9.14)=21.42$, $p=0.001$, $\eta p^2=0.704$	$F(1.53,13.74)=2.66$, $p=0.115$, $\eta p^2=0.228$
Station-count CV	$F(1.03,9.26)=69.67$, $p<0.001$, $\eta p^2=0.886$	$F(1.16,10.43)=8.41$, $p=0.013$, $\eta p^2=0.483$
P10 throughput	$F(1.00,9.01)=2.76$, $p=0.131$, $\eta p^2=0.235$	$F(1.06,9.54)=5.11$, $p=0.047$, $\eta p^2=0.362$
Zero-throughput ratio	$F(1.00,9.00)=1.00$, $p=0.343$, $\eta p^2=0.100$	$F(1.94,17.47)=0.71$, $p=0.502$, $\eta p^2=0.073$
Serving RSSI	$F(1.22,10.96)=59.90$, $p<0.001$, $\eta p^2=0.869$	$F(1.74,15.70)=0.27$, $p=0.736$, $\eta p^2=0.029$

Outcome	Association×Density
Aggregate throughput	$F(1.13,10.13)=2.37$, $p=0.154$, $\eta p^2=0.208$
Packet loss	$F(1.98,17.79)=7.10$, $p=0.006$, $\eta p^2=0.441$
Jain fairness	$F(1.61,14.52)=1.28$, $p=0.300$, $\eta p^2=0.124$
Station-count CV	$F(1.98,17.83)=1.68$, $p=0.215$, $\eta p^2=0.157$
P10 throughput	$F(1.21,10.87)=1.94$, $p=0.193$, $\eta p^2=0.177$
Zero-throughput ratio	$F(1.00,9.00)=1.00$, $p=0.343$, $\eta p^2=0.100$
Serving RSSI	$F(2.12,19.11)=3.27$, $p=0.057$, $\eta p^2=0.267$

3.7 Per-AP Delivered-Throughput Balance

Table 5. Supplementary station-count and per-AP delivered-throughput balance (five paired seeds)

STA	Policy	Station-count CV	AP throughput CV	Agg. Mbps	Jain
50	RSSI	0.452	0.077	144.49	0.660
50	LOAD	0.102	0.088	142.89	0.766
50	HYBRID	0.160	0.079	144.46	0.772
70	RSSI	0.374	0.060	145.68	0.703
70	LOAD	0.063	0.063	144.66	0.773
70	HYBRID	0.107	0.054	146.39	0.780

Table 5 uses paired seeds 1–5, a subset of the main experiment's seeds 1–10. With saturated downlink traffic, continuously backlogged APs may operate near their configuration-dependent limits despite different association counts, plausibly explaining the low AP-throughput CV across policies. At 50 STAs, AP-throughput CV was 0.077 (RSSI), 0.088 (LOAD), and 0.079 (HYBRID); at 70 STAs, it was 0.060, 0.063, and 0.054, respectively. No AP-throughput-CV contrast was significant after Holm correction. The larger CV under the supplementary On-Off test (Table 6) cannot be attributed solely to traffic because MAC processing also differed. These findings do not establish traffic-model causality or policy equivalence.

3.8 Bidirectional Bursty-Traffic Robustness Check

Table 6. Supplementary bidirectional bursty On-Off robustness check at 50 STAs (three paired seeds)

Policy	Total Mbps	DL Mbps	UL Mbps	DL Jain	AP DL-throughput CV
RSSI	87.77	68.10	19.68	0.750	0.373
LOAD	94.84	75.42	19.42	0.795	0.227
HYBRID	95.87	76.31	19.56	0.798	0.211

Under bidirectional bursty traffic (Table 6), mean total delivered throughput was 87.77 Mbps for RSSI, 94.84 Mbps for LOAD, and 95.87 Mbps for HYBRID. Mean downlink Jain fairness was 0.750, 0.795, and 0.798, and AP downlink-throughput CV was 0.373, 0.227, and 0.211. The ordering matches the load-aware interpretation of the main benchmark, but no paired contrast reached $p<0.05$ after Holm correction. With only three paired seeds, this is presented as descriptive robustness evidence and not as confirmatory inference.

4. Discussion

Aggregate throughput rose with station density and then stayed at roughly 145–149 Mbps beyond 30 STAs, even as packet loss and lower-tail user throughput worsened. The plateau is a saturation result for this 2.4 GHz/20 MHz, fixed-MCS, full-buffer configuration. It does not show that the deployment would cope with arbitrary demand. The three association rules worked on the same physical links and channels, so their clearest differences lie in which stations get service and how users are divided among APs, not in the throughput ceiling.

Across the ten paired seeds, HYBRID exceeded strongest-RSSI association in mean Jain fairness at 30, 50, and 70 STAs, by about 0.103–0.168, while the association effect on aggregate throughput was not significant (p=0.111). A non-significant effect does not establish throughput equivalence. Earlier work connects association decisions with load distribution and fairness [6,7], and the more recent studies [10-12] address related resource-allocation questions. Bejerano et al. expressed fairness in max-min terms, and the network settings of both [6] and [7] differ from the present one, so their numerical values cannot be compared directly with the Jain index reported here. The direction of the effect is nevertheless the same: in the present simulations, accounting for load reduced the concentration of users on a subset of APs and gave a more even distribution of throughput. The fairness gain should not be read as extra physical channel capacity in this fixed deployment. The AP-load results are in line with the motivation behind AP-selection metrics that look beyond signal strength, such as potential bandwidth [5] and channel measurements [8]. HYBRID reduced CV_{load} by more than 60% relative to RSSI at 30–70 STAs, and pure LOAD reduced it further at the two highest densities. This improvement came with a radio-link trade-off. Strongest-RSSI association preserved the best mean signal level, pure LOAD accepted the weakest links, and HYBRID occupied an intermediate point. Balancing load and maximizing link quality therefore pull in different directions. In the present configuration, the most useful operating point lay between maximizing signal strength and minimizing AP occupancy.

Adame et al. reported throughput and delay gains when RSSI was combined with access and backhaul load in a home Wi-Fi architecture [9]. No comparable gain in aggregate throughput was found here. Their topology, load metric and backhaul assumptions differ from the present fixed four-AP, downlink-saturated setup, which may explain the difference. In the current experiment, load awareness manifested primarily as better fairness and AP balance rather than a statistically significant increase in total throughput. The benefit of a load-aware method is therefore likely to depend on which resource limits performance in the modeled network. Full-buffer traffic can mask differences in per-AP delivered throughput: continuously backlogged APs may approach configuration-dependent service limits despite unequal association counts. Low AP-throughput CV therefore does not establish equal offered load or airtime. At 50 STAs, LOAD had lower station-count CV than RSSI, but AP-throughput CV values were similar (0.088 versus 0.077); at 70 STAs, HYBRID had the lowest AP-throughput CV (0.054), without a significant paired contrast. Table 6

shows larger CV under bursty traffic, but also used a different MAC processing mode. These five-seed findings support cautious interpretation, not a definitive throughput-balance claim.

Density, not association policy, dominated the loss of service quality. At 70 STAs, the mean application-layer non-delivery ratio approached 0.62 for every policy and about 15% of users received no throughput; together with the fall in P10 throughput, these findings support the description of functional congestion collapse under the saturated fixed-rate configuration. The throughput plateau hides this: added users do not bring proportional delivered capacity, while lower-tail throughput collapses and loss climbs. Calling the state graceful capacity sharing would understate how badly service fails. The zero-throughput users also bear on the word “optimized.” The preceding ACO stage optimized spatial RF coverage, not multi-user load, adaptive-rate performance, or per-user service guarantees, and its 95.2% simulated coverage and 3.0% dead-zone fraction (computed with its own propagation model) cannot guarantee non-zero throughput for every randomly placed client in a fixed-MCS saturated network. In the diagnostic 10-STA RSSI run, the three zero-throughput users had serving RSSI of −73.70, −80.24, and −84.81 dBm and a packet-loss ratio of 1.0. With MCS fixed at 4 and link adaptation off, a weak link cannot drop to a lower MCS. The observation is consistent with weak-link outage, although the data do not show that RSSI alone caused each failure. Fixing MCS 4 removed rate adaptation as a confounding factor, but it also makes the zero-throughput metric more severe than it would be for a real client able to switch to a more robust MCS. The ratio is an outage-like outcome of the controlled fixed-rate configuration, not a field estimate of indoor coverage probability. Such outages lower Jain fairness and raise mean packet loss whatever the association policy. Rate control also interacts with the spatial-reuse mechanisms of IEEE 802.11ax in dense deployments [30]. The remedies are therefore physical and operational: joint placement-association optimization, additional APs in persistently weak areas, adaptive rate control, and coordinated channel planning are more promising than changes to association alone.

The sensitivity analysis also limits what the BIM propagation model can support. The 50 dB/m fallback for unmapped foam segments can create localized artificial shadowing. Replacing it with 1–3 dB/m changed the mean RSSI at the original serving AP by only about 0.17–0.20 dB, yet 4.23% of LOAD and 3.13% of HYBRID association decisions differed from the baseline. The preceding placement stage used its own propagation model with different material parameters, so its coverage figures cannot be transferred to the benchmark without recomputation. ITU-R P.2040 and measurements such as [17,18] support the dependence of transmission and reflection on material and frequency, but not these numerical coefficients. Calibration against material-specific measurements would strengthen the physical interpretation. A second limitation is geometric. The model computes the 3D AP-STA distance and rejects wall intersections outside a wall's vertical extent, but wall penetration uses the orthogonal layer thickness and omits incidence-angle path extension, angle-dependent reflection, diffraction, floor and ceiling reflections, and explicit multipath. The 4.0 m AP height follows the BIM ceiling plane. It was not optimized in the placement stage and was not checked against field mounting heights. All three policies share these choices, which keeps the comparison like for like but limits absolute RF realism. The foam sensitivity analysis also showed that LOAD and HYBRID decisions respond more to the tested foam-loss assumption than strongest-RSSI decisions do.

Uniform random users were kept as a neutral paired baseline, which avoids building a hotspot around one AP. Real occupancy is usually clustered by room function, though, and clustered or hotspot demand could widen the gap between LOAD and HYBRID when one AP is disproportionately loaded. Mobility would add re-association and handover overhead that is absent here. The bidirectional On-Off test narrows the traffic-model limitation without removing it: the same qualitative ordering appeared in the three sampled topologies under one On-Off condition, but the policies have not been validated for web, video, VoIP, or mobile clients. The study also uses a single building geometry and a single four-AP layout, and the abstract PHY does not reproduce every waveform-level impairment [23,24]. The use of BIM also differs from earlier work. Foundational indoor-propagation studies have shown the value of walls, floors and building layout in site-specific prediction [13,14], while more recent BIM-based work has demonstrated that 3D geometry and building semantics can support Wi-Fi propagation and AP-placement analyses [20-

22]. The present work uses BIM differently: the physical deployment is held fixed and the BIM-derived environment is used as the radio context for a system-level load experiment. In this way, building-informed RF modeling is linked with operational WLAN resource management, two topics that the studies cited here address separately.

For these four fixed APs, association changed how service was distributed more clearly than how much aggregate throughput was delivered. HYBRID gave higher user fairness and much lower count imbalance than strongest-RSSI association at medium and high densities and kept stronger serving links than pure LOAD, but it did not lead on every metric, and neither load-aware policy removed weak-link outages or the high-loss regime at 70 STAs. A layout that covers most locations is therefore not necessarily sufficient for heavily loaded fixed-rate operation, which matters for how the preceding RF-coverage optimization should be read.

5. Conclusions

This study evaluated RSSI, load-aware, and hybrid AP association after a four-AP indoor deployment had been fixed by a BIM-based RF-coverage optimization. “Optimized” therefore refers only to that coverage objective, not to multi-user throughput, fixed-MCS outage, or end-to-end service. The main experiment comprised 120 paired-topology IEEE 802.11ax simulations with 10, 30, 50, and 70 static stations under a deliberately controlled 2.4 GHz/20 MHz, fixed-MCS-4, downlink full-buffer configuration.

Association policy did not significantly alter aggregate throughput in the main benchmark (p=0.111). Above 30 STAs, throughput stayed at roughly 145–149 Mbps, which is read as a saturation ceiling of this configuration and not as deployment resilience. The informative differences were in resource distribution: HYBRID gave significantly higher Jain fairness than RSSI at 30, 50, and 70 STAs and substantially reduced imbalance in associated-station counts. Pure LOAD gave the lowest count imbalance but the weakest mean serving RSSI, and HYBRID sat between LOAD and RSSI, about 2 dB weaker than RSSI and 1.4–1.8 dB stronger than LOAD at 30–70 STAs. In the five-seed supplementary per-AP analysis, delivered-throughput CV remained low under all policies despite differing station-count CV values, as can occur with continuously backlogged APs. No AP-throughput-CV contrast remained significant; these results neither demonstrate equivalent AP throughput nor establish that station-count balancing independently changes delivered-traffic balance. Station count should be treated only as a simplified association-load proxy. User density caused the most serious degradation. At 70 STAs, mean application-layer packet non-delivery was about 62% and the zero-throughput ratio about 15% under every policy, while P10 throughput fell to a few hundredths of a megabit per second. Under the saturated fixed-rate benchmark this is a functional congestion collapse, not a benign redistribution of a stable capacity. The zero-throughput results fit the scope of the preceding placement stage: it optimized RF coverage, not multi-user contention, adaptive rate selection, or per-user service guarantees. Association control alone cannot repair persistent weak-link areas or a physical capacity shortage, so joint placement-association optimization, additional APs, adaptive MCS selection, and coordinated channel planning are natural extensions.

Two robustness checks refine these conclusions. Replacing the high foam fallback with low-loss bounds changed mean RSSI only slightly but altered about 3–4% of LOAD and HYBRID association decisions, so material-loss assumptions can affect threshold-based load-aware decisions within the tested model. A three-seed bidirectional On-Off experiment retained the descriptive policy ordering, with HYBRID highest in mean delivered throughput and fairness and lowest in AP downlink-throughput CV. Because full MAC replaced the main benchmark’s MAC frame abstraction, and only three seeds were used, this finding is neither causal nor confirmatory. With AP locations, channels, MCS, and offered load held fixed, load-aware association improved some measures of user-level allocation without a significant gain in aggregate throughput. Whether these differences persist remains to be tested with calibrated BIM wall losses, realistic AP heights, angular and multipath propagation effects, clustered or mobile users, adaptive link rates, and application-specific traffic. Placement, association, and channel selection should then be assessed jointly across the 2.4, 5, and 6 GHz bands, instead of assuming that coverage optimization alone provides

adequate service capacity. Field experiments with controlled numbers of active clients would also strengthen external validation, and the fallback wall elements and the assumed AP height should be replaced by verified material and installation data when available.

Nomenclature

Symbol	Definition
AP	Access point
STA	Station/client
RSSI	Received signal strength indicator
MCS	Modulation and coding scheme
PL	Path loss (dB)
PL_{total}, $PL_{distance}$	Total path loss and distance-dependent path loss (dB)
L_w	Penetration loss of crossed wall w (dB)
f_c	Channel center frequency (GHz)
d	3D transmitter-receiver distance (m)
$I(\cdot)$	Indicator function (one if the condition holds, otherwise zero)
a_l	Effective attenuation coefficient for material layer l (dB/m)
t_l	Orthogonal thickness of material layer l (m)
w, l	Wall index, material-layer index
L_j	Number of STAs associated with AP j, station-count load proxy
CV_{load}	Coefficient of variation of associated-station counts
$CV_{throughput}$	Coefficient of variation of per-AP delivered throughput
J	Jain fairness index
α	Weight of the normalized RSSI term in HYBRID scoring
i; j, k	Station index, AP indices
AP_i^*	AP selected for station i under RSSI association
$RSSI_{ij}$	Received signal strength of AP j at station i (dBm)
$RSSI_{min}$, $RSSI_{max}$	Lower and upper RSSI bounds used for normalization (−70 and −30 dBm)
R_{ij}^{norm}	Normalized RSSI score of AP j for station i
L_j^{norm}	Normalized station-count load of AP j
S_{ij}	HYBRID selection score of AP j for station i
n	Number of STAs
T_i	Throughput of station i (Mbps)
B_i	Application-layer bytes received by station i
t	Simulation duration (s)
σ_L, $\bar{L}$	Sample standard deviation and mean of L_j across the four APs
θ	Angle of incidence (not modeled)

References

[1] Bellalta B. IEEE 802.11ax: High-efficiency WLANs. IEEE Wireless Communications, 2016;23(1):38-46. https://doi.org/10.1109/MWC.2016.7422404

[2] Khorov E, Kiryanov A, Lyakhov A, Bianchi G. A tutorial on IEEE 802.11ax high efficiency WLANs. IEEE Communications Surveys & Tutorials, 2019;21(1):197-216. https://doi.org/10.1109/COMST.2018.2871099

[3] Deng DJ, Lin YP, Yang X, Zhu J, Li YB, Luo J, Chen KC. IEEE 802.11ax: Highly efficient WLANs for intelligent information infrastructure. IEEE Communications Magazine, 2017;55(12):52-59. https://doi.org/10.1109/MCOM.2017.1700285

[4] Mozaffariahrar E, Theoleyre F, Menth M. A survey of Wi-Fi 6: Technologies, advances, and challenges. Future Internet, 2022;14(10):293. https://doi.org/10.3390/fi14100293

[5] Vasudevan S, Papagiannaki K, Diot C, Kurose J, Towsley D. Facilitating access point selection in IEEE 802.11 wireless networks. Internet Measurement Conference 2005 (IMC 2005), Berkeley, CA, USA, 293-298, 2005. https://doi.org/10.1145/1330107.1330141

[6] Bejerano Y, Han SJ, Li L. Fairness and load balancing in wireless LANs using association control. IEEE/ACM Transactions on Networking, 2007;15(3):560-573. https://doi.org/10.1109/TNET.2007.893680

[7] Gong H, Kim JW. Dynamic load balancing through association control of mobile users in WiFi networks. IEEE Transactions on Consumer Electronics, 2008;54(2):342-348. https://doi.org/10.1109/TCE.2008.4560097

[8] Hong K, Kim JP, Kim MS, Lee S. Channel measurement-based access point selection in IEEE 802.11 WLANs. Pervasive and Mobile Computing, 2016;30:58-70. https://doi.org/10.1016/j.pmcj.2015.10.018
[9] Adame T, Carrascosa M, Bellalta B, Pretel I, Etxebarria I. Channel load aware AP/Extender selection in Home WiFi networks using IEEE 802.11k/v. IEEE Access, 2021;9:30095-30112. https://doi.org/10.1109/ACCESS.2021.3059473
[10] Ak E, Canberk B. QoS-aware load balancing scheme in dense Wi-Fi 6 WLANs. Industrial Networks and Intelligent Systems - 8th EAI International Conference, INISCOM 2022, Lecture Notes of the Institute for Computer Sciences, Social-Informatics and Telecommunications Engineering 444, 33-47, 2022. https://doi.org/10.1007/978-3-031-08878-0_3
[11] Zhang L, Yin H, Roy S, Cao L, Gao X, Sathya V. IEEE 802.11be network throughput optimization with multilink operation and AP controller. IEEE Internet of Things Journal, 2024;11(13):23850-23861. https://doi.org/10.1109/JIOT.2024.3386653
[12] Shao S, Wang Z, Xu S, Guo S, Qiu X. Multi-AP cooperative radio resource allocation method for co-channel interference avoidance in 802.11be WLAN. Computers, Materials & Continua, 2025;84(3):4949-4972. https://doi.org/10.32604/cmc.2025.065053
[13] Seidel SY, Rappaport TS. 914 MHz path loss prediction models for indoor wireless communications in multifloored buildings. IEEE Transactions on Antennas and Propagation, 1992;40(2):207-217. https://doi.org/10.1109/8.127405
[14] Seidel SY, Rappaport TS. Site-specific propagation prediction for wireless in-building personal communication system design. IEEE Transactions on Vehicular Technology, 1994;43(4):879-891. https://doi.org/10.1109/25.330150
[15] International Telecommunication Union. Propagation data and prediction methods for the planning of indoor radiocommunication systems and radio local area networks in the frequency range from 300 MHz to 450 GHz. Recommendation ITU-R P.1238-13, Geneva, ITU, 2025.
[16] International Telecommunication Union. Effects of building materials and structures on radio-wave propagation in the range of 1 MHz to 450 GHz. Recommendation ITU-R P.2040-4, Geneva, ITU, 2025.
[17] Bytyqi S, Jashari B. Experimental assessment of the effects of building materials on Wi-Fi signal 2.4 GHz and 5 GHz. Journal of Computer and Communications, 2024;12:1-10. https://doi.org/10.4236/jcc.2024.125001
[18] Koppel T, Shishkin A, Haldre H, Toropovs N, Vilcane I, Tint P. Reflection and transmission properties of common construction materials at 2.4 GHz frequency. Energy Procedia, 2017;113:158-165. https://doi.org/10.1016/j.egypro.2017.04.045
[19] Ramírez-Arroyo A, Damsgaard SB, Berardinelli G, Sørensen TB, Mogensen P, Kaagaard J. Wi-Fi 6E mesh networks: Where to place the extenders? 2024 IEEE 100th Vehicular Technology Conference (VTC2024-Fall), Washington DC, USA, 1-7, 2024. https://doi.org/10.1109/VTC2024-Fall63153.2024.10757459
[20] Cheng JCP, Li KCT. Developing a BIM-assisted 3D access point placement optimization algorithm for enhancing Wi-Fi fingerprint-based indoor positioning. Computing in Civil Engineering 2019: Visualization, Information Modeling, and Simulation, Atlanta, GA, USA, 232-240, 2019. https://doi.org/10.1061/9780784482421.030
[21] Hosseini H, Taleai M, Zlatanova S. NSGA-II based optimal Wi-Fi access point placement for indoor positioning: A BIM-based RSS prediction. Automation in Construction, 2023;152:104897. https://doi.org/10.1016/j.autcon.2023.104897
[22] Pan H, Huang Z, Zheng W. Virtual fingerprint indoor localization based on signal propagation model: RSS prediction using BIM. Journal of Building Engineering, 2025;113:113752. https://doi.org/10.1016/j.jobe.2025.113752
[23] The MathWorks Inc. Overview of WLAN system-level simulation. MATLAB R2026b Documentation [Internet]. Natick, MA: The MathWorks Inc.; 2026 [cited 2026 Oct 27]. Available from: https://www.mathworks.com/help/wlan/ug/overview-of-wlan-system-level-simulation.html
[24] IEEE 802.11 Task Group ax. 11ax evaluation methodology. IEEE 802.11-14/0571r12. IEEE; 2016.
[25] IEEE 802.11 Task Group ax. TGax simulation scenarios. IEEE 802.11-14/0980r16. IEEE; 2015.
[26] Jain R, Chiu DM, Hawe WR. A quantitative measure of fairness and discrimination for resource allocation in shared computer systems. DEC Research Report TR-301. Digital Equipment Corporation; 1984.
[27] National Institute of Standards and Technology. Coefficient of variation. Dataplot Reference Manual [Internet]. Gaithersburg, MD: NIST; [cited 2026 Oct 27]. Available from: https://itl.nist.gov/div898/software/dataplot/refman2/auxillar/coefvari.htm
[28] Greenhouse SW, Geisser S. On methods in the analysis of profile data. Psychometrika, 1959;24(2):95-112. https://doi.org/10.1007/BF02289823
[29] Holm S. A simple sequentially rejective multiple test procedure. Scandinavian Journal of Statistics, 1979;6(2):65-70.
[30] Krotov A, Kiryanov A, Khorov E. Rate control with spatial reuse for Wi-Fi 6 dense deployments. IEEE Access, 2020;8:168898-168909. https://doi.org/10.1109/ACCESS.2020.3023552